

# Inferring Pore Connectivity from Sorption Hysteresis in Multiscale Porous Media

Matthew B. Pinson<sup>a</sup>, Tingtao Zhou<sup>a</sup>, Hamlin M. Jennings<sup>b,1</sup>, Martin Z. Bazant<sup>c</sup>

<sup>a</sup>*Department of Physics, Massachusetts Institute of Technology*

<sup>b</sup>*Department of Civil and Environmental Engineering, Massachusetts Institute of Technology*

<sup>c</sup>*Department of Chemical Engineering and Mathematics, Massachusetts Institute of Technology*

---

## Abstract

### *Hypothesis*

Vapor adsorption experiments are widely used to assess pore size distributions, but the large hysteresis sometimes observed between sorption and desorption isotherms remains difficult to interpret. Such hysteresis is influenced by pore network connectivity, which has previously been modeled by percolation on infinite lattices. Our hypothesis is that percolation occurs instead through finite networks of micropores connecting accessible macropores, always exposed to the outside environment.

### *Theory*

We derive a general formula for sorption/desorption isotherms that introduces a simple measure of hierarchical pore connectivity – the fraction  $f$  of always exposed pores. The model thus accounts for “small world” connections in finite-size percolation, while also incorporating other hysteresis mechanisms, in single-pore filling, liquid insertion into the solid matrix, and cavitation.

### *Findings*

Our formula is able to fit and interpret both primary and scanning sorption/desorption isotherms for a variety of adsorbates (noble gases, water,

---

<sup>1</sup>Deceased in July 2015. R.I.P.

and organics) and porous materials (cement pastes, dental enamels, porous glasses, carbon black and nanotubes), including cases with broad pore-size distributions and large hysteresis. It allows quantification of the prevalence of percolating macropores in the material, even though these pores are never filled during the sorption experiments. A distinct bump in sorption isotherms is explained as a lowering of the barrier to nucleation of the vapor phase with a universal temperature scaling.

*Keywords:* vapor adsorption, capillary condensation, sorption/desorption isotherms, hysteresis, porous media, connectivity, percolation

---

## 1. Introduction

The properties of a porous material, such as strength, permeability and hydrodynamic dispersion, depend on the structure of both the solid matrix and the pore space. Although various standard experimental methods are available [15], the geometry and topology of the pore network can be difficult to characterize experimentally, especially due to the wide range of length scales, which can extend below one nanometer. A standard characterization approach is vapor adsorption, in which the partial pressure of an adsorbate is varied and the sorbed mass (or the intensity of a nuclear magnetic resonance signal [1]) measured. In principle, such measurements enable quantification of the internal surface area, the pore size distribution (PSD), and to some extent the connectivity of the pore network.

One important aspect in the interpretation of sorption isotherms is the widely-observed hysteresis between adsorption and desorption isotherms [2], and any valid model of sorption must account for this hysteresis. Analytical and numerical models have been developed [3, 4, 5, 6, 7, 8, 9], where several mechanisms of hysteresis on different scales have been identified: 1) chemical effects on the molecular scale 2) single pore hysteresis on the scale of individual pores and 3) pore-blocking or ink-bottle effect on the scale of pore networks. When bottleneck sizes are smaller than a certain critical value, cavitation happens before the bottlenecks become empty, and modifies the shape of the hysteresis loop [10, 11]. In this article we are mainly concerned with the case where the solid matrix of the porous media is fully wetted by the adsorbate, thus minimizing the importance of contact angle hysteresis [12, 13, 14, 15]. This mechanism is important in non-wetting solid-liquid contacts such as mercury porosimetry, though it still does not explain all the

hysteresis in that case[12, 16].

We extend the existing infinite-lattice percolation models [4, 5, 17, 18, 19, 20] in combination with single pore hysteresis and cavitation, and propose a new parameter  $f$ , characterizing always-exposed large pores and representing the finite-size effect of samples. We show that this parameter varies among different types of hierarchical porous materials. We first review different hysteresis mechanisms and identify their importance in different types of hysteresis. Of particular interest are multiscale materials, where the PSD is very wide and percolation effects are beyond the explanation of a single threshold size. We show that sorption hysteresis in such materials is heavily influenced by network effects, where  $f$ , in addition to the coordination number  $z$ , plays an important role. The partial pressure of cavitation inferred from the sorption isotherm hysteresis shows the trend predicted by theoretical models. The inferred order parameter  $f$ , together with PSD can be used in further material modeling. For instance, a better understanding of the prevalence of large and small pores and how they are connected will be beneficial to the modeling of transport in porous media [21], since transport processes are much faster in larger pores. Such transport modeling is applicable to a wide variety of problems, including creep and corrosion in concrete [22], capture of carbon dioxide in sorbents such as zeolites or activated carbon [23], and shale gas extraction [24].

## 2. Single pore hysteresis

### 2.1. Surface adsorption

One mode by which a gas can be sorbed by a mesoporous material is adsorption on pore walls. Numerous isotherms have been proposed to describe the average thickness of the adsorbed layer as a function of partial pressure, of which the Langmuir [25] and BET [26] equations are best known. The Langmuir equation is based on the assumption that only a monolayer can adsorb, while the BET equation uses the opposite assumption that an infinite number of layers can adsorb, with no lateral interaction between adsorbed molecules. Although adsorption is likely to fall somewhere between these extremes, we use the BET equation for simplicity. The BET equation [26] gives the average thickness of the adsorbed layer, in units of a monolayer, as

$$t_m(h) = \frac{ch}{[(c-1)h+1](1-h)}. \quad (1)$$

Here  $h$  is the relative pressure of the sorbate, i.e., its partial pressure divided by its saturation pressure. The constant  $c$ , usually determined empirically, is related to the strength of the interaction between the sorbate and the solid surface.

The validity of the BET equation has been questioned due to its neglect of lateral forces between adsorbed molecules within each layer [27, 28, 29]. However, it is successfully and very widely used to explain experimental results [30, 31, 32]. It may be that, although lateral forces are present, they mostly act to reduce variations in layer thickness without substantially impacting the average adsorbed quantity. Also, interactions between the solid surface and layers above the first may increase the number of layers in which lateral interactions are unimportant. We model surface adsorption by the BET equation in this work and reasonable results are obtained.

## 2.2. Pore filling

In addition to adsorption on pore walls, the sorbate can condense within the mesopores. The relationship between a radius  $r$  of a liquid-vapor interface located within a pore and the relative pressure at which the full and empty (we refer to a pore containing no condensed fluid as empty, although it still has adsorbed fluid on its pore walls) states are in equilibrium is given by the Kelvin equation [33, 34, 35]:

$$\ln h = \frac{\alpha \gamma a^3}{rkT}. \quad (2)$$

Here  $\gamma$  is the liquid-vapor surface tension,  $a^3$  is the average volume per molecule in the condensed state,  $k$  is the Boltzmann constant and  $T$  is temperature. The use of the Kelvin equation relies on the assumption that a continuum treatment of water is valid down to small length scales, as suggested by the explanation of freezing point suppression by an analogous continuum equation [36]. The prefactor  $\alpha$  accounts for the shape of the liquid-vapor interface. For example, in cylindrical pores, during adsorption the liquid film grows radially inward but during desorption the liquid-vapor meniscus recedes along the cylinder axis, causing a different prefactor ( $\alpha = 1$  for adsorption,  $\alpha = 2$  for desorption) and hence hysteresis even for a single cylindrical pore [3, 37, 38]. Figure 1 illustrates these processes. The situation of a slit pore is even more extreme: the mean radius of curvature when the pore is full is equal to the distance between the adsorbed layers on the pore walls, but since there is no pre-existing curvature the pore will not fill

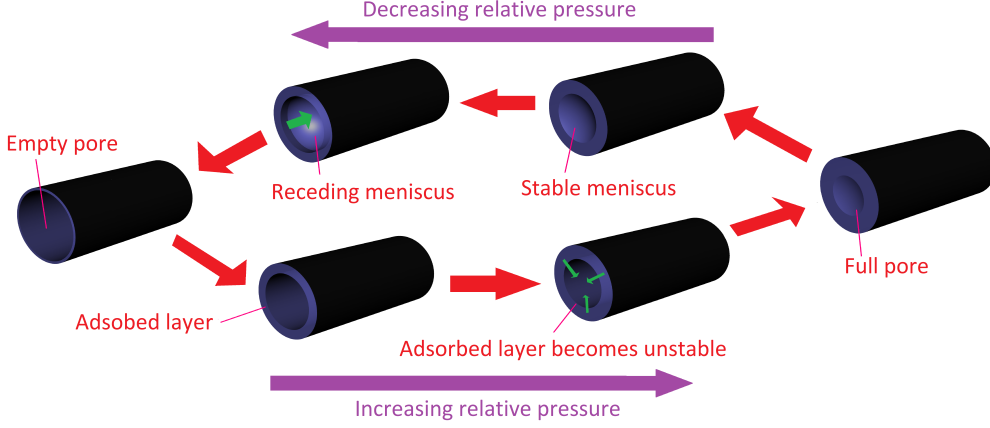


Figure 1: A schematic illustration of radial filling during wetting (bottom) and axial emptying during drying (top).

until the adsorbed layers grow so thick that they touch. In realistic material structures the Kelvin prefactor difference between adsorption and desorption will be further influenced by 3D geometry.

This mechanism is sufficient to describe materials with simple pore structure where network effects are negligible, such as dichlorofluoromethane in plugs of carbon black [39], shown in Fig. 2a. During drying, the cylindrical pore starts as fully saturated, and its meniscus resembles a hemisphere which has non-zero Gaussian curvature. Only when the relative pressure goes below a critical value will the meniscus start to recede and the pore empty. For an ensemble of different sizes of independent pores, given relative pressure  $h$ , pores larger than a critical radius will have unstable meniscus and become empty. We denote this critical radius as  $r_{eq}$ , defined by

$$r_{eq}(h) = \frac{2\gamma a^3}{kT \ln h} + at_m(h) \quad (3)$$

We denote it as the “equilibrium desorption radius” to emphasize that the liquid inside is in direct contact with the external vapor phase through the meniscus interface, so the meniscus interface is free to propagate or recede and eventually arrives at an “equilibrium” spatial position. This is in contrast to the situation where the pore is blocked by other smaller pores. In that case its meniscus interface can be held at the pore boundary instead of receding and disappearing, which would happen if it were not blocked. We

will elaborate again on this difference in Section 4. If the distribution of pore radii  $r$ , by pore volume, is  $v(r)$ , the sorbed volume at relative pressure  $h$  during drying is

$$m_d(h) = \int_0^{r_{eq}(h)} v(r) dr + \int_{r_{eq}(h)}^{\infty} \frac{r^2 - [at_m(h)]^2}{r^2} v(r) dr, \quad (4)$$

The first term accounts for all pores small enough to already be filled at  $h$ , the second term for the large pores that remain empty but contribute through their surface layer adsorption.

During wetting, a pore remains empty until the relative pressure rises above a threshold which we refer to as the filling pressure. Given  $h$ , all pores smaller than  $r_{fill}(h)$  will be full:

$$r_{fill}(h) = \frac{\gamma a^3}{kT \ln h} + at_m(h) \quad (5)$$

. Notice the prefactor differs by a factor of 2 between  $r_{eq}$  and  $r_{fill}$  for cylindrical pores, hence hysteresis is produced. This hysteresis arises from differences in the shape of the meniscus during filling and emptying. The total sorbed liquid volume during wetting is then

$$m_w(h) = \int_0^{r_{fill}(h)} v(r) dr + \int_{r_{fill}(h)}^{\infty} \frac{r^2 - [at_m(h)]^2}{r^2} v(r) dr, \quad (6)$$

The meaning of the two terms are similar to the drying case, except that the critical radius  $r_{fill}$  is different from  $r_{eq}$ .

### 3. Insertion within the “solid”

Equations 4 and 6 describe sorption in mesopores. Many porous materials possess a hierarchical pore structure, and sorbate can be found not only in the mesopores, but also in even smaller spaces within what would be considered the “solid” part of the structure [40] [41]. Simple models that treat the sorbate as a condensing fluid are not applicable to these very small (approximately one nanometer or smaller) spaces, because they neglect strong chemical interactions with the sorbent material, as well as effects arising due to the discreteness of the sorbate molecules [42]. One approach is to use various atomistic simulation techniques [43]. We note that in a material such

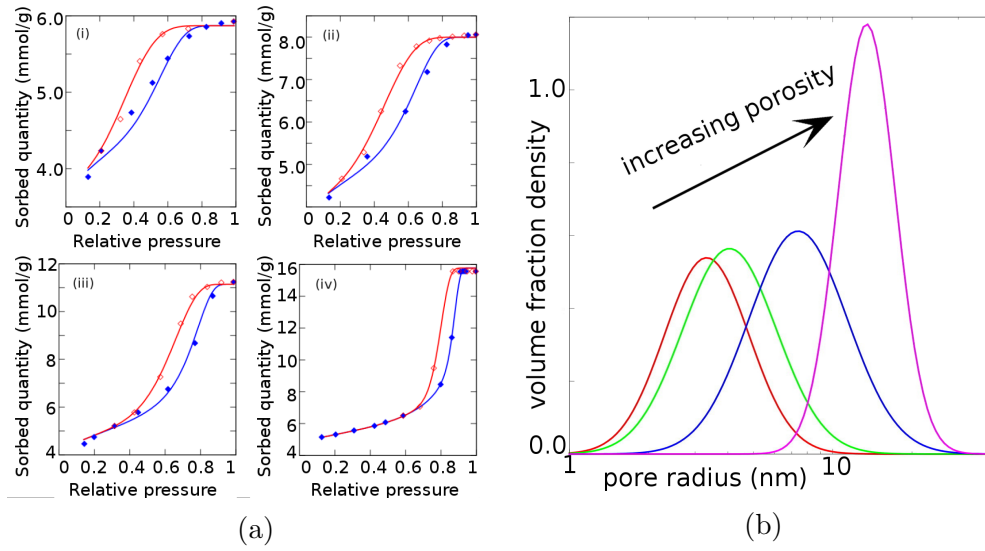


Figure 2: Sorption hysteresis explained by single pore filling in of dichlorofluoromethane in carbon black [39]. (a) Experimental sorption isotherms (points) for wetting (blue) and drying (red). Subfigures with porosity of (i) 0.50, (ii) 0.58, (iii) 0.66 and (iv) 0.74. Lines are the analytical results of single pore hysteresis. (b) Pore size distributions obtained by assuming cylindrical pores with only single pore filling hysteresis.

as cement paste in which inserted water (known as interlayer water [44]) is particularly important, the inserted water content as a function of relative humidity is well approximated by assuming no loss of water on drying until 15% relative humidity is reached, linear loss of water below this, and linear reinsertion on wetting [45, 46, 47, 48]. Thus we only treat the amount of inserted water at complete saturation as a unknown parameter in this work.

#### 4. Network effects

The single pore hysteresis mechanism, accounting for hysteresis due to differences in the shape of the liquid-vapor interface in an isolated pore on wetting and drying, can accurately describe sorption in particular porous materials, with nearly independent pores. In a system with a wide range of pore sizes and good pore connectivity, network effects can act to broaden hysteresis. The additional hysteresis is due to some pores remaining full below the relative pressure at which the empty state is thermodynamically favored, because they lack the connection with the vapor phase that is necessary to nucleate the liquid to vapor transition. This is frequently known as “pore blocking” [6, 9, 11], though it is worth noticing that the effect is not based on kinetics but purely on consideration of local equilibrium. Figure 3 illustrates this effect for a toy system comprising two cylindrical pores.

Various models of this hysteresis have been developed, applicable to certain types of pore network but not universally. Mason [5] proposed a model of pores connected by windows, each with a characteristic radius drawn from a distribution [17]. Parlar and Yortsos [49] extended this model to more completely describe the case of scanning isotherms. Seaton [50] applied the model to the calculation of the average coordination number of pores in various materials, while Tanev and Vlaev [6] considered the relationship between assumptions about the pore shape and the corresponding hysteresis loop.

The models presented in the above articles focus primarily on the percolation threshold. They assume that no emptying of a significant number of pores occurs until the vapor region is able to percolate through this network. This assumption seems to work well for materials where the pore size distribution is not too wide, such as porous glass [17]. An interesting and not fully addressed scenario is when the material, with a broad PSD, has a fraction of large pores empty at the start of desorption, immediately below the saturation pressure. This could be because these pores are so large that they do not fill until relative humidity approaches very close to 1 in the experiments,



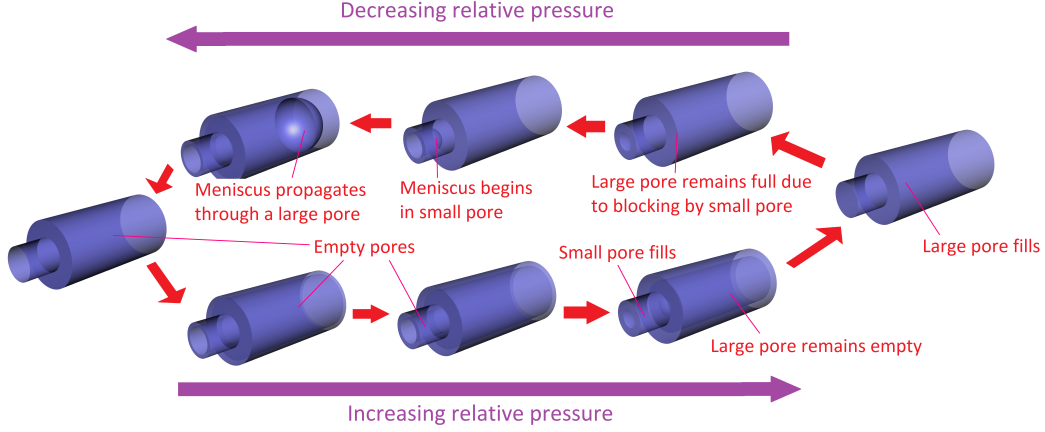


Figure 3: Illustration of a system comprising a large pore whose only path to the atmosphere passes through a small pore, exposed to a cycle of relative pressure. The large pore remains full until the small pore empties and provides a meniscus where the liquid-vapor transition can be nucleated.

or because they are able to empty without hindrance due to a connection to a continuous network of large pores, in which case evaporation can be much more efficient due to the "small world" effect [51, 52, 53].

Since the network provides a hindrance only to drying, the sorbate content during wetting is the same as that in the independent pore model given in Eqn. 6. The desorption branch can be calculated by mean-field percolation models [17, 18, 19, 20], summarized as following. Assuming cylindrical pores, at a particular relative pressure  $h$ , the fraction  $q$  of pores that are below their emptying transition pressure, referred to as a "large pore", is given by

$$q = \frac{\int_{r_{eq}(h)}^{\infty} \frac{v(r)}{r^2} dr}{\int_0^{\infty} \frac{v(r)}{r^2} dr}. \quad (7)$$

The total sorbed volume during drying will then be

$$m_d(h) = \int_0^{r_{eq}(h)} v(r) dr + (1-Q) \int_{r_{eq}(h)}^{\infty} v(r) dr + Q \int_{r_{eq}(h)}^{\infty} \frac{r^2 - [r - at_m(h)]^2}{r^2} v(r) dr, \quad (8)$$

where  $Q$  is the probability of such a large pore being actually empty. Various lattices can be chosen such as simple cubic [18] or a Bethe lattice with coordination number  $z$  [5, 50] and  $Q$  can be calculated based on the lattice choice.

However, no single infinite-lattice model without finite size effects can adequately describe both simple pore structures such as those of Vycor glass or silica gel, and more hierarchical pore networks such as in cement paste or dental enamel. We extend and generalize the percolation models by introducing a parameter  $f$ , defined to be the fraction of all pores exposed to a liquid-vapor interface as soon as drying commences, so that the pores empty as soon as their equilibrium transition pressure is reached. The exposure may, for instance, be due to a connection to a very large percolating pore that remains empty, as illustrated in Fig. 4, and these always exposed pores bring in the boundary effect of an effectively finite lattice. There are thus two mechanisms by which a particular pore may have access to the vapor phase. The first is direct exposure, with probability  $f$ . The second is that it could be connected to the vapor by a neighbor on the lattice. We denote  $X$  to be the probability that an individual neighbor provides such a connection. We then can write

$$1 - Q = (1 - f)(1 - X)^z. \quad (9)$$

Due to the self-similarity of the Bethe lattice, we can further write

$$X = q[f + (1 - f)(1 - (1 - X)^{z-1})]. \quad (10)$$

We solve equation 10 self-consistently to find  $X$ , and then use equation 9 to calculate  $Q$ .

## 5. Cavitation

One further effect controls desorption at low relative pressure. This effect has been called cavitation [54, 11] or the tensile strength effect [55]. The cause of desorption is that the condensed fluid becomes unstable at sufficiently low pressure, without direct exposure to a vapor phase.

We assume that the primary result of this desorption mechanism is the homogeneous nucleation of the vapor phase in blocked large pores. The pressure at which confined cavitation [56] or spinodal decomposition [57, 58] occurs in a pore of width  $r_n$  can be derived as

$$h_n(r_n) = h_n(\infty)e^{-\frac{2\gamma v}{[r_n - at(h_n)]kT}}, \quad (11)$$

where  $h_n(\infty)$  is a parameter in the model, with a value that depends on the sorbate and temperature but not on the sorbent. This gives a relationship

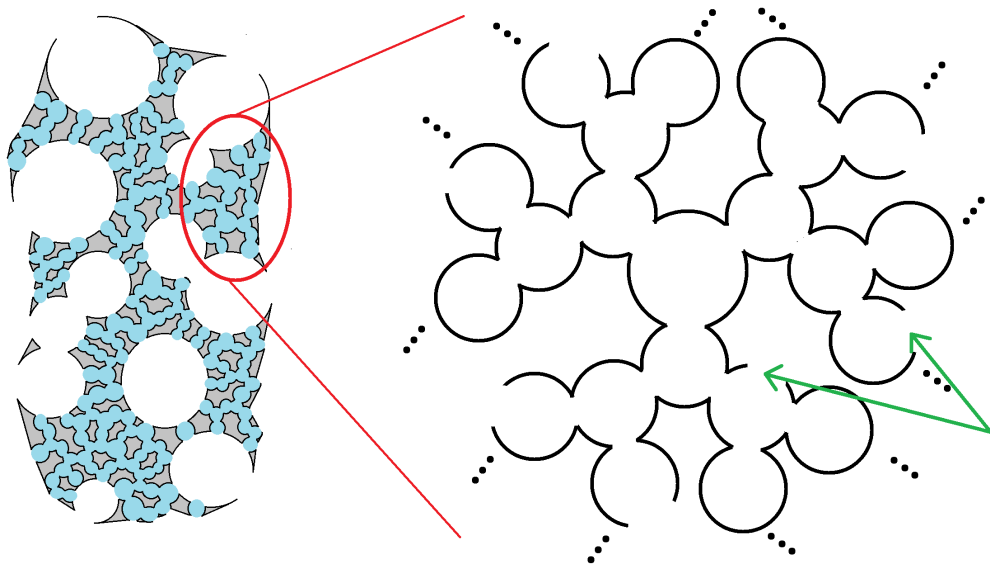


Figure 4: A schematic diagram of a hierarchical network of small (blue) and larger always exposed (white) pores formed by a solid skeleton (grey), and its representation by a modified Bethe lattice, visualized with  $z = 3$ . The holes in some of the displayed pores, noted by green arrows, represent an interface between the network of small pores and larger pores that are always exposed and acting as a finite boundary to the originally infinite Bethe lattice.

between relative pressure and the width above which all pores must be empty. If we define

$$q_n = \frac{\int_{r_n}^{\infty} \frac{v(r)}{r^2} dr}{\int_0^{\infty} \frac{v(r)}{r^2} dr}, \quad (12)$$

we can then write

$$X = q_n + (q - q_n)[f + (1 - f)(1 - (1 - X)^{z-1})] \quad (13)$$

and

$$\begin{aligned} m_d(h) = & \int_0^{r_{eq}(h)} v(r) dr + (1 - Q) \int_{r_{eq}(h)}^{r_n} v(r) dl \\ & + Q \int_{r_{eq}(h)}^{r_n} \frac{r^2 - [r - at_m(h)]^2}{r^2} v(r) dr + \int_{r_n}^{\infty} \frac{r^2 - [r - at_m(h)]^2}{r^2} v(r) dr. \end{aligned} \quad (14)$$

## 6. Results of the extended finite-size percolation model

### 6.1. Adsorption/desorption isotherms and values for $f$

Figure 5a compares our extended model results with experimental observations for various systems [59, 60, 61, 62]. The model parameters were determined in each case by a least squares fit. To avoid overfitting, we fix the value of  $z = 4$  throughout this study for all materials concerned, focusing on the new order parameter  $f$  proposed here. Figure 6a shows the calculated pore size distributions for these materials. The median radius of 13 nm found for the case of carbon nanotubes is consistent with the transmission electron microscope image of these nanotubes (figure 12 of [60]).

Values of  $f$  calculated for various materials are summarized in table 1. Uncertainty ranges are calculated by comparing isotherms of samples produced with different specifications (hardened cement paste), or taken at different temperatures (dental enamel) or using different sorbates (porous silica glass and Vycor). This is statistical uncertainty only and does not account for model uncertainty. The calculated  $f$  values indicate that the finite size effect of percolation lattice model is more significant for some hierarchical porous materials such as cement paste and enamel than other materials such as Vycor and silica glass. The percolating large pores in these systems with higher  $f$  values are expected to have prominent effects on the sorption isotherm,

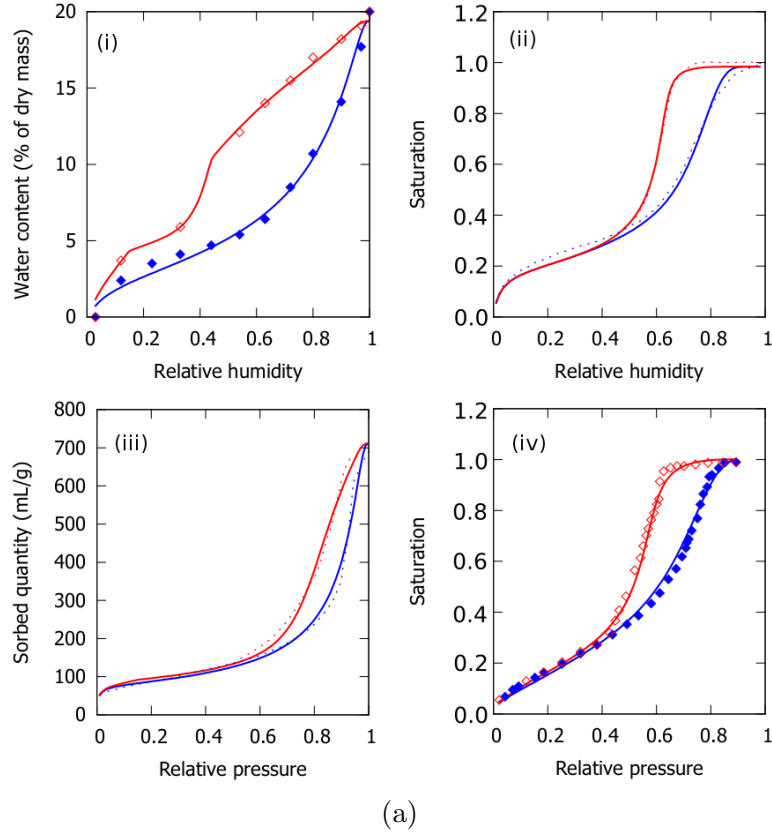


Figure 5: Extended model applied on various materials. Calculated sorption isotherms (lines), along with experimental isotherms (points or dashed lines) for wetting (blue) and drying (red) of (i) water in hardened cement paste [59], (ii) water in Vycor [61], (iii) nitrogen in carbon nanotubes [60] and (iv) xenon in silica glass [62].

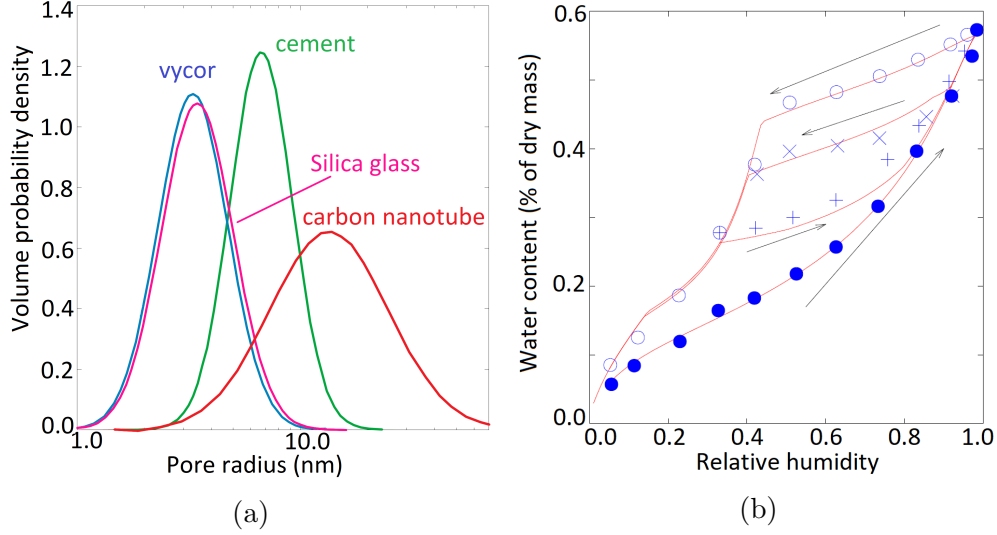


Figure 6: Extended model applied on various materials. (a) Volume density function for hardened cement paste [59], Vycor [61], carbon nanotubes [60] and silica glass [62]. (b) Primary and scanning sorption isotherms calculated using the model of this work (solid lines), along with experimental primary (circles) and scanning (crosses) sorption isotherms for water in dental enamel at 298 K [63].

consistent with other studies [64, 65]. Further direct measurements of the  $f$  values in these systems will be very interesting to compare with the presented model.

### 6.2. Scanning isotherms

The principles of the model can be applied directly to the case of scanning isotherms, where the partial pressure is cycled over some subsection of the possible range.

If the decrease in partial pressure is halted at  $h_-$  and the partial pressure then increased to  $h$ , the total sorbed volume will be

$$\begin{aligned}
 m_{\uparrow scan}(h) = & \int_0^{r_K(h_-)+at(h_-)} v(r) dr + [1 - Q(h_-)] \int_{r_K(h_-)+at(h_-)}^{r_n(h_-)} v(r) dr \\
 & + Q(h_-) \int_{r_K(h_-)+at(h_-)}^{r_n(h_-)} \frac{r^2 - [r - at_m(h)]^2}{r^2} v(r) dr \\
 & + \int_{r_n(h_-)}^{\infty} \frac{r^2 - [r - at_m(h)]^2}{r^2} v(r) dr,
 \end{aligned}$$

Table 1: Fraction of always exposed pores,  $f$ , calculated by applying the model presented here to a variety of published experimental data.

Material	Sorbate/s	Reference	$f$
CNT	N <sub>2</sub>	[60]	0.40
Cement	H <sub>2</sub> O	[66] [59]	$0.33 \pm 0.06$
Enamel	H <sub>2</sub> O	[63]	$0.54 \pm 0.05$
Silica glass	Xe, C <sub>4</sub> H <sub>10</sub> CCl <sub>2</sub> F <sub>2</sub> , O <sub>2</sub>	[62]	$0.13 \pm 0.09$
Vycor	N <sub>2</sub>	[67]	$0.06 \pm 0.01$
	H <sub>2</sub> O	[61]	
	C <sub>6</sub> H <sub>14</sub>	[68]	

where any non-zero integral bound must be replaced by  $r_{fill}(h)$  when the latter surpasses the former.

If the increase in partial pressure is halted at  $h_+$  and the partial pressure then decreased to  $h$ , the total sorbed mass can be calculated using equations 12 and 4, but using the smaller of  $r_n(h)$  and  $r_K(h_+)/2 + at(h_+)$  in place of  $r_n(h)$ , i.e. the radius of the largest pores that could be filled.

Figure 6b compares the model with experimental scanning isotherms for dental enamel [63].

### 6.3. Prediction of liquid cavitation pressure

Liquid cavitation and fracture under tensile stress has long been a topic of interest [69, 70, 71, 72, 73]. One tantalising prospect is the use of experiments like those cited in this work to measure the bulk cavitation relative pressure  $h_n(\infty)$  for various fluids as a function of temperature. In only two distinct cases, water around 25 °C and at 50 °C, was the characteristic knee observed.  $h_n(\infty)$  was larger at higher temperature as expected. A systematic study could allow this quantity to be measured as a function of temperature, providing insight into the nature of forces between molecules in a liquid. For example, the regular solution model [57] predicts

$$h_\infty = \frac{e^{-2\sqrt{1-\tau}/\tau}(1 + \sqrt{1-\tau})}{1 - \sqrt{1-\tau}}, \quad (15)$$

where  $\tau = T/T_c$  is temperature divided by the critical temperature of the sorbate (reduced temperature). Likewise, a universal curve can be obtained

for a Van der Waals gas, though there is no simple analytic form. The independence of the curves on material specifics suggests that there is a general trend across sorbates. Figure 7 compares available points found using the model, in which  $h_n(\infty)$  depends on sorbate and temperature but not sorbent, with the theoretical curves of regular solution model and Van der Waals gas.

## 7. Discussion

Based on our analysis of physical mechanisms for sorption hysteresis, we present a theoretical modeling approach to investigate pore connectivity from sorption hysteresis experiments. The model presented provides an overall description of hysteresis sorption in mesoporous media, especially in materials in which macropores are also present. The existence and connectivity of these macropores are characterized by an parameter  $f$  describing the prevalence of large pores, in addition to the average pore coordination number  $z$ . We calculate pore size distribution and connectivity for various materials, predict scanning isotherms and compare them to experiment data. Bulk liquid cavitation pressure can be inferred as a parameter in our model controlling the existence and position of the desorption knee. We find the bulk cavitation relative pressure for water increases with increasing temperature, using the best fit values from our model calculation on water sorption data. Theoretical curves given by the regular solution model and Van der Waals liquid predict a similar trend, with the regular solution model quantitatively closer to our results. More direct experiment data on bulk liquid rupture will help validate the models.

Nevertheless, there remain some complications that increase the uncertainty in the level to which the model can quantitatively describe pore size and network structure. First, the model as formulated assumes cylindrical pores, and a particular amount of single-pore hysteresis due to differences in the shape of the liquid-vapor interface. Other assumptions, such as slit pores with larger hysteresis or equilibrium filling and hence no hysteresis, could have been made instead and built into the model in a straightforward way. Agreement with TEM observations for the case of carbon nanotubes gives some confidence that the assumption of cylindrical pores is reasonable. However, the assumption still influences the obtained results. Specifically, if cylindrical pores are assumed when the system is really made up of slit pores, the obtained pore sizes will be larger and obtained value of  $f$  smaller than



in reality (the discrepancies are opposite if in fact the pores are able to reach local equilibrium on filling). Second, the model uses a very simple model of surface adsorption. The effect of this can be seen in some discrepancy between model and experimental results at low pressure. Where the data are available, this could be rectified by using experimental  $t$  curves, at the loss of some generality. Third, the assumption of a fixed value of  $z$  precludes distinguishing between systems based on their connectivity. For example, we might expect carbon nanotubes to have  $z \approx 2$ , while disordered porous systems such as glasses and cement paste have higher  $z$ . Sorption data alone are not sufficient to allow such an identification to be made. Also, it seems to be  $f$  rather than  $z$  that is most influential in determining the sorption behavior.

The modeling approach here has been used in previous studies on cement sorption, drying shrinkage and creep [64, 74, 75], where the multiscale porous structure of cement paste exemplifies a high  $f$  value, and a distinct bump on the desorption branch at around 40 % relative humidity exists due to cavitation. The good comparison with cement sorption and shrinkage data demonstrates the power of this physics based theoretical model.

The model has the potential to contribute to transport modeling not only through its assessment of connectivity, but also by identifying and explaining the hysteresis in the sorbed mass as a function of local sorbate chemical potential. Existing models of transport in porous materials do not account for this hysteresis, simplified by defining an effective diffusivity  $D(S)$  [76, 77] by

$$\frac{\partial S}{\partial t} = \nabla \cdot [D(S) \nabla S], \quad (16)$$

where  $S$  is the local saturation of sorbate. Although this can give a qualitative idea of the conditions under which transport is faster or slower, more accurate transport rate can be determined with knowledge of local chemical potential gradients, which can be calculated through a model such as the one presented here. Deeper understanding of the transport processes will assist in the design of these materials with desired transport properties. The transport of water and of ions dissolved in the water is also highly relevant to degradation and contamination in concrete [78, 79, 80] and many other materials [81, 82].

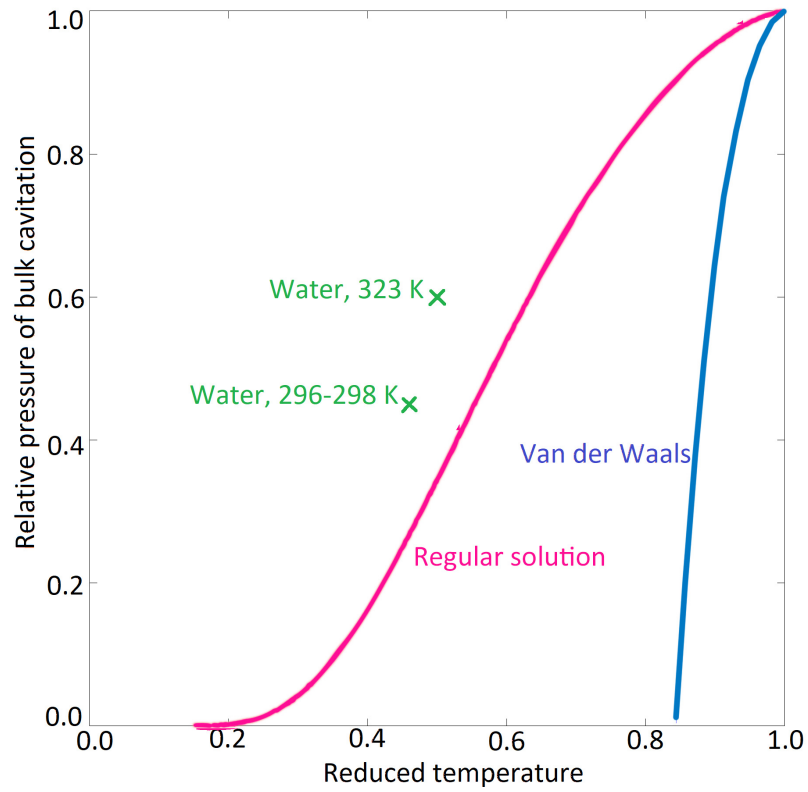


Figure 7: Partial pressure at which the vapor phase is nucleated in the bulk, as a function of reduced temperature. Points denote values obtained by applying the model of this work to experimental data, while the solid lines are the results of the regular solution and van der Waals models.

## 8. Conclusions

The hysteresis in adsorption/desorption isotherms caused by the collective effect within a pore network has been mainly modeled by idealized infinite lattice percolation models[4, 5, 17, 18, 19, 20]. We present an extension to these percolation models by introducing a parameter  $f$  characterizing the fraction of always exposed large pores, effectively incorporating boundary effects of percolation on a finite size lattice. Our calculated  $f$  values indicate the importance of finite size percolation effects in different materials. The model is simplified with certain assumptions as discussed above, nevertheless it addresses the currently missing link between 3D simulations of colloidal systems and macroscopic continuum models of vapor sorption, and provides a pathway to overcome the current empirical treatment of sorption isotherms in continuum poromechanical models [83, 84, 85, 86].

The significant bump in the desorption isotherm, which typically appears in multiscale materials such as cement paste, around 40% relative pressure in the case of water at 25 °C, can be well explained by an effect of cavitation (equivalently, homogeneous nucleation). The pressure at which this bump is located in experimental data varies with temperature in a trend consistent with theoretical expectations, though available data are limited.

The development here of an extended model relating macroscopic sorption behavior to microstructure can assist the design of materials for applications such as moisture buffering [87], and the understanding of the dependence of thermal conductivity on water content [88]. Since connectivity plays a vital role in determining the transport properties of a material [89, 90], it would be very interesting for future research to examine the relationship between  $f$  and  $z$  and the permeability to single-phase flow. More generally, for multiphase flow in porous media, this could lead to improved mathematical models of the relative permeability and capillary pressure [16], which also exhibit strong and poorly understood hysteresis.

This work was supported by the Concrete Sustainability Hub at MIT with sponsorship provided by the Portland Cement Association (PCA) and the Ready Mixed Concrete (RMC) Research & Education Foundation, and by the National Science Foundation via an EAGER Collaborative Grant #1153509. The authors acknowledge useful discussions with the members of the Dome collaboration and G. Sant.

## References

- [1] A. C. A. Muller, K. L. Scrivener, A. M. Gajewicz, P. J. McDonald, Densification of CSH Measured by  $^1\text{H}$  NMR Relaxometry, *The Journal of Physical Chemistry C* 117 (1) (2013) 403–412. doi:10.1021/jp3102964. URL <http://pubs.acs.org/doi/abs/10.1021/jp3102964>
- [2] K. S. W. Sing, D. H. Everett, R. A. W. Haul, L. Moscou, R. A. Pierotti, J. Rouquerol, T. Siemieniewska, Reporting physisorption data for gas/solid systems with special reference to the determination of surface area and porosity, *Pure & Applied Chemistry* 57 (4) (1985) 603–619. URL <http://jpkc2.wzu.edu.cn/clwlhx/uploadfile/201012/20101221013858456.pdf>
- [3] L. H. Cohan, Sorption hysteresis and the vapor pressure of concave surfaces, *Journal of the American Chemical Society* 60 (2) (1938) 433–435. URL <http://pubs.acs.org/doi/abs/10.1021/ja01269a058>
- [4] G. Mason, The effect of pore space connectivity on the hysteresis of capillary condensation in adsorption-desorption isotherms, *Journal of Colloid and Interface Science* 88 (1) (1982) 36–46. doi:10.1016/0021-9797(82)90153-9. URL <http://linkinghub.elsevier.com/retrieve/pii/0021979782901539>
- [5] G. Mason, A model of adsorption-desorption hysteresis in which hysteresis is primarily developed by the interconnections in a network of pores, *Proceedings of the Royal Society of London. A.* 390 (1983) 47–72. URL <http://rspa.royalsocietypublishing.org/content/390/1798/47.short>
- [6] P. T. Tanev, L. T. Vlaev, An attempt at a more precise evaluation of the approach to mesopore size distribution calculations depending on the degree of pore blocking, *Journal of Colloid and Interface Science* 160 (1993) 110–116. URL <http://www.sciencedirect.com/science/article/pii/S0021979783713743>

- [7] H. Liu, L. Zhang, N. A. Seaton, Sorption Hysteresis as a Probe of Pore Structure, *Langmuir* 9 (1993) 2576–2582.
- [8] F. Rojas, I. Kornhauser, C. Felipe, J. M. Esparza, S. Cordero, A. Domínguez, J. L. Riccardo, Capillary condensation in heterogeneous mesoporous networks consisting of variable connectivity and pore-size correlation, *Physical Chemistry Chemical Physics* 4 (11) (2002) 2346–2355. doi:10.1039/b108785a.  
URL <http://xlink.rsc.org/?DOI=b108785a>
- [9] P. I. Ravikovitch, A. V. Neimark, Experimental confirmation of different mechanisms of evaporation from ink-bottle type pores: equilibrium, pore blocking, and cavitation, *Langmuir* 18 (10) (2002) 9830–9837.  
URL <http://pubs.acs.org/doi/abs/10.1021/la026140z>
- [10] C. Fan, D. Do, D. Nicholson, On the cavitation and pore blocking in slit-shaped ink-bottle pores, *Langmuir* 27 (7) (2011) 3511–3526.
- [11] M. Thommes, K. Kaneko, A. V. Neimark, J. P. Olivier, F. Rodriguez-Reinoso, J. Rouquerol, K. S. Sing, Physisorption of gases, with special reference to the evaluation of surface area and pore size distribution (iupac technical report), *Pure and Applied Chemistry* 87 (9-10) (2015) 1051–1069.
- [12] H. Giesche, Mercury porosimetry: a general (practical) overview, *Particle & particle systems characterization* 23 (1) (2006) 9–19.
- [13] J. H. Caro, H. Freeman, Physical structure of fertilizer materials, pore structure of phosphate rock and triple superphosphate, *Journal of Agricultural and Food Chemistry* 9 (3) (1961) 182–186.
- [14] C. Salmas, G. Androustopoulos, Mercury porosimetry: Contact angle hysteresis of materials with controlled pore structure, *Journal of colloid and interface science* 239 (1) (2001) 178–189.
- [15] S. Lowell, J. E. Shields, M. A. Thomas, M. Thommes, Characterization of porous solids and powders: surface area, pore size and density, Vol. 16, Springer Science & Business Media, 2012.

- [16] Z. Gu, M. Z. Bazant, Microscopic theory of capillary pressure hysteresis based on pore-space accessivity and radius-resolved saturation, in preparation.
- [17] G. Mason, Determination of the Pore-Size Distributions and Pore-Space Interconnectivity of Vycor Porous Glass from Adsorption-Desorption Hysteresis Capillary Condensation Isotherms, *Proceedings of the Royal Society A: Mathematical, Physical and Engineering Sciences* 415 (1849) (1988) 453–486. doi:10.1098/rspa.1988.0023.  
URL <http://rspa.royalsocietypublishing.org/cgi/doi/10.1098/rspa.1988.0023>
- [18] H. Liu, L. Zhang, N. A. Seaton, Analysis of sorption hysteresis in mesoporous solids using a pore network model, *Journal of colloid and interface science* 156 (2) (1993) 285–293.
- [19] H. Liu, N. A. Seaton, Determination of the connectivity of porous solids from nitrogen sorption measurements-III. Solids containing large mesopores, *Chemical Engineering Science* 49 (11) (1994) 1869–1878.  
URL <http://www.sciencedirect.com/science/article/pii/0009250994800715>
- [20] A. Neimark, Percolation theory of capillary hysteresis phenomena and its application for characterization of porous solids, in: *Studies in Surface Science and Catalysis*, Vol. 62, Elsevier, 1991, pp. 67–74.
- [21] F. A. L. Dullien, *Porous Media Fluid Transport and Pore Structure*, 2nd Edition, Academic Press, San Diego, 1992.
- [22] L. Bertolini, B. Elsener, P. Pedferri, R. Polder, *Corrosion of Steel in Concrete Prevention, Diagnosis, Repair*, Wiley-VCH, Weinheim, 2004.
- [23] S. Choi, J. H. Drese, C. W. Jones, Adsorbent materials for carbon dioxide capture from large anthropogenic point sources., *ChemSusChem* 2 (9) (2009) 796–854. doi:10.1002/cssc.200900036.  
URL <http://www.ncbi.nlm.nih.gov/pubmed/19731282>
- [24] F. Javadpour, D. Fisher, M. Unsworth, Nanoscale Gas Flow in Shale Gas Sediments, *Journal of Canadian Petroleum Technology* 46 (10) (2007) 55–61. doi:10.2118/07-10-06.

URL <http://www.onepetro.org/mslib/servlet/onepetropreview?id=PETSOC-07-10-06&soc=PETSOC>

- [25] I. Langmuir, The constitution and fundamental properties of solids and liquids. Part I. Solids, *Journal of the Franklin Institute* 38 (11) (1917) 2221–2295.  
URL <http://pubs.acs.org/doi/abs/10.1021/ja02268a002>
- [26] S. Brunauer, P. H. Emmett, E. Teller, Adsorption of gases in multi-molecular layers, *Journal of the American Chemical Society* 60 (1938) 309–319.  
URL <http://pubs.acs.org/doi/abs/10.1021/ja01269a023>
- [27] K. Sing, The use of nitrogen adsorption for the characterisation of porous materials, *Colloids and Surfaces A: Physicochemical and Engineering Aspects* 187–188 (2001) 3–9. doi:10.1016/S0927-7757(01)00612-4.  
URL <http://linkinghub.elsevier.com/retrieve/pii/S0927775701006124>
- [28] A. Seri-Levy, D. Avnir, The Brunauer-Emmett-Teller equation and the effects of lateral interactions. A simulation study, *Langmuir* 9 (10) (1993) 2523–2529. doi:10.1021/la00034a009.  
URL <http://pubs.acs.org/doi/abs/10.1021/la00034a009>
- [29] M. Z. Bazant, Z. P. Bažant, Theory of sorption hysteresis in nanoporous solids: Part II Molecular condensation, *Journal of the Mechanics and Physics of Solids* 60 (2012) 1660–1675.  
URL <http://www.sciencedirect.com/science/article/pii/S0022509612000968>
- [30] F. M. Nelsen, F. T. Eggertsen, Determination of surface area. adsorption measurements by continuous flow method, *Analytical Chemistry* 30 (8) (1958) 1387–1390.  
URL <http://pubs.acs.org/doi/abs/10.1021/ac60140a029>
- [31] M. Bhambhani, P. Cutting, K. Sing, D. Turk, Analysis of nitrogen adsorption isotherms on porous and nonporous silicas by the BET and  $\alpha$ s methods, *Journal of Colloid and Interface Science* 38 (1) (1972) 109–117. doi:10.1016/0021-9797(72)90226-3.

- URL <http://linkinghub.elsevier.com/retrieve/pii/0021979772902263>
- [32] P. J. Branton, P. G. Hall, K. S. W. Sing, Physisorption of nitrogen and oxygen by MCM-41, a model mesoporous adsorbent, *Journal of the Chemical Society, Chemical Communications* (1993) 1257–1258.  
URL <http://pubs.rsc.org/en/content/articlepdf/1993/c3/c39930001257>
  - [33] E. P. Barrett, L. G. Joyner, P. P. Halenda, The determination of pore volume and area distributions in porous substances. i. computations from nitrogen isotherms, *Journal of the American Chemical society* 73 (1) (1951) 373–380.
  - [34] W. Thomson, 4. on the equilibrium of vapour at a curved surface of liquid, *Proceedings of the Royal Society of Edinburgh* 7 (1872) 63–68.
  - [35] T. Stifter, O. Marti, B. Bhushan, Theoretical investigation of the distance dependence of capillary and van der waals forces in scanning force microscopy, *Physical Review B* 62 (20) (2000) 13667.
  - [36] S. Shimizu, Exploring Transport, Adsorption and Phase Behavior in Nanoporous Materials Final Progress Report, Tech. rep., Massachusetts Institute of Technology, Cambridge (2014).
  - [37] J. C. P. Broekhoff, J. H. De Boer, Studies on Pore Systems in Catalysts IX. Calculation of pore distributions from the adsorption branch of nitrogen sorption isotherms in the case of open cylindrical pores A. Fundamental equations, *Journal of Catalysis* 9 (1967) 8–14.  
URL <http://www.sciencedirect.com/science/article/pii/0021951767901741>
  - [38] F. Celestini, Capillary condensation within nanopores of various geometries, *Physics Letters A* 228 (1-2) (1997) 84–90.  
doi:10.1016/S0375-9601(97)00070-4.  
URL <http://linkinghub.elsevier.com/retrieve/pii/S0375960197000704>
  - [39] P. C. Carman, F. A. Raal, Physical Adsorption of Gases on Porous Solids. I. Comparison of Loose Powders and Porous Plugs, *Proceedings*



- of the Royal Society A: Mathematical, Physical and Engineering Sciences 209 (1096) (1951) 59–69. doi:10.1098/rspa.1951.0187.  
URL <http://rspa.royalsocietypublishing.org/cgi/doi/10.1098/rspa.1951.0187>
- [40] I. G. Richardson, Tobermorite/jennite- and tobermorite/calcium hydroxide-based models for the structure of C-S-H: applicability to hardened pastes of tricalcium silicate,  $\beta$ -dicalcium silicate, Portland cement, and blends of Portland cement with blast-furnace slag, metakaol, Cement and Concrete Research 34 (9) (2004) 1733–1777. doi:10.1016/j.cemconres.2004.05.034.  
URL <http://linkinghub.elsevier.com/retrieve/pii/S0008884604002364>
- [41] I. Richardson, The calcium silicate hydrates, Cement and Concrete Research 38 (2) (2008) 137–158. doi:10.1016/j.cemconres.2007.11.005.  
URL <http://linkinghub.elsevier.com/retrieve/pii/S0008884607002876>
- [42] Z. P. Bažant, M. Z. Bazant, Theory of sorption hysteresis in nanoporous solids: Part I Snap-through instabilities, Journal of the Mechanics and Physics of Solids 60 (9) (2012) 1644–1659. doi:10.1016/j.jmps.2012.04.014.  
URL <http://linkinghub.elsevier.com/retrieve/pii/S0022509612000956>
- [43] P. A. Bonnaud, B. Coasne, R. J.-M. Pellenq, Molecular simulation of water confined in nanoporous silica., Journal of Physics: Condensed Matter 22 (28) (2010) 284110. doi:10.1088/0953-8984/22/28/284110.  
URL <http://www.ncbi.nlm.nih.gov/pubmed/21399282>
- [44] G. L. Kalousek, Fundamental factors in the drying shrinkage of concrete block, Journal of the American Concrete Institute 26 (3) (1954) 233–248.  
URL <http://www.concrete.org/Publications/InternationalConcreteAbstractsPortal.aspx?m=details&i=11675>
- [45] R. F. Feldman, Helium flow characteristics of rewetted specimens of dried hydrated Portland cement paste, Cement and Concrete Research

- 3 (1973) 777–790.  
 URL <http://www.sciencedirect.com/science/article/pii/S0008884673900112>
- [46] H. M. Jennings, Refinements to colloid model of C-S-H in cement: CM-II, *Cement and Concrete Research* 38 (3) (2008) 275–289. doi:10.1016/j.cemconres.2007.10.006.  
 URL <http://linkinghub.elsevier.com/retrieve/pii/S0008884607002761>
- [47] A. C. A. Muller, K. L. Scrivener, A. M. Gajewicz, P. J. McDonald, Use of bench-top NMR to measure the density, composition and desorption isotherm of C-S-H in cement paste, *Microporous and Mesoporous Materials* 178 (2013) 99–103. doi:10.1016/j.micromeso.2013.01.032.  
 URL <http://linkinghub.elsevier.com/retrieve/pii/S1387181113000620>
- [48] P. Bonnaud, Q. Ji, B. Coasne, R.-M. Pellenq, K. Van Vliet, Thermodynamics of water confined in porous calcium-silicate-hydrates, *Langmuir* 28 (31) (2012) 11422–11432.
- [49] M. Parlar, Y. C. Yortsos, Percolation theory of vapor adsorption-desorption processes in porous materials, *Journal of Colloid and Interface Science* 124 (1) (1988) 162–176.  
 URL <http://www.sciencedirect.com/science/article/pii/S0021979788903372>
- [50] N. A. Seaton, Determination of the connectivity of porous solids from nitrogen sorption measurements, *Chemical Engineering Science* 46 (8) (1991) 1895–1909. doi:10.1016/0009-2509(91)80151-N.  
 URL <http://linkinghub.elsevier.com/retrieve/pii/S000925099180151N>
- [51] C. Moore, M. E. Newman, Epidemics and percolation in small-world networks, *Physical Review E* 61 (5) (2000) 5678.
- [52] D. J. Watts, S. H. Strogatz, Collective dynamics of small-world networks, *nature* 393 (6684) (1998) 440.
- [53] V. Latora, M. Marchiori, Efficient behavior of small-world networks, *Physical review letters* 87 (19) (2001) 198701.

- [54] M. Thommes, B. Smarsly, M. Groenewolt, P. I. Ravikovitch, A. V. Neimark, Adsorption hysteresis of nitrogen and argon in pore networks and characterization of novel micro- and mesoporous silicas., *Langmuir* 22 (2) (2006) 756–764. doi:10.1021/la051686h.  
URL <http://www.ncbi.nlm.nih.gov/pubmed/16401128>
- [55] J. C. Groen, L. A. A. Peffer, J. Perez-Ramirez, Pore size determination in modified micro- and mesoporous materials. Pitfalls and limitations in gas adsorption data analysis, *Microporous and Mesoporous Materials* 60 (2003) 1–17. doi:10.1016/S1387-1811(03)00339-1.  
URL <http://linkinghub.elsevier.com/retrieve/pii/S1387181103003391>
- [56] C. J. Rasmussen, A. Vishnyakov, M. Thommes, B. M. Smarsly, F. Kleitz, A. V. Neimark, Cavitation in metastable liquid nitrogen confined to nanoscale pores, *Langmuir* 26 (12) (2010) 10147–10157.
- [57] J. H. Hildebrand, A quantitative treatment of deviations from raoult’s law, *Proceedings of the National Academy of Sciences* 13 (5) (1927) 267–272.
- [58] M. Z. Bazant, Theory of chemical kinetics and charge transfer based on nonequilibrium thermodynamics, *Accounts of chemical research* 46 (5) (2013) 1144–1160.
- [59] V. Baroghel-Bouny, Water vapour sorption experiments on hardened cementitious materials part I: essential tool for analysis of hygral behaviour and its relation to pore structure, *Cement and Concrete Research* 37 (3) (2007) 414–437. doi:10.1016/j.cemconres.2006.11.019.  
URL <http://linkinghub.elsevier.com/retrieve/pii/S0008884606003115>
- [60] E. Frackowiak, F. Béguin, Carbon materials for the electrochemical storage of energy in capacitors, *Carbon* 39 (6) (2001) 937–950. doi:10.1016/S0008-6223(00)00183-4.  
URL <http://linkinghub.elsevier.com/retrieve/pii/S0008622300001834>
- [61] J.-C. Li, D. K. Ross, M. J. Benham, Small-angle neutron scattering studies of water and ice in porous Vycor glass, *Journal of Applied*

Crystallography (1991) 794–802.

URL <http://scripts.iucr.org/cgi-bin/paper?S0021889891001929>

- [62] W. D. Machin, Temperature dependence of hysteresis and the pore size distributions of two mesoporous adsorbents, *Langmuir* (May 1993) (1994) 1235–1240.  
URL <http://pubs.acs.org/doi/abs/10.1021/1a00016a042>
- [63] R. T. Zahradnik, E. C. Moreno, Structural Features of Human Dental Enamel as Revealed by Isothermal Water Vapour Sorption, *Archives of Oral Biology* 20 (1975) 317–325.
- [64] M. B. Pinson, E. Masoero, P. A. Bonnaud, H. Manzano, Q. Ji, S. Yip, J. J. Thomas, M. Z. Bazant, K. J. Van Vliet, H. M. Jennings, Hysteresis from multiscale porosity: modeling water sorption and shrinkage in cement paste, *Physical Review Applied* 3 (6) (2015) 064009.
- [65] K. Ioannidou, K. J. Krakowiak, M. Bauchy, C. G. Hoover, E. Masoero, S. Yip, F.-J. Ulm, P. Levitz, R. J.-M. Pellenq, E. Del Gado, Mesoscale texture of cement hydrates, *Proceedings of the National Academy of Sciences* 113 (8) (2016) 2029–2034.
- [66] R. F. Feldman, Sorption and length-change scanning isotherms of methanol and water on hydrated Portland cement, in: *V International Symposium on the Chemistry of Cement*, Volume 3, 1968, pp. 53–66.  
URL <http://scholar.google.com/scholar?hl=en&btnG=Search&q=intitle:Sorption+and+Length-Change+Scanning+Isotherms+of+Methanol+and+Water+on+Hydrated+Portland+Cement#0>
- [67] D. F. Brewer, D. C. Champeney, Sorption of helium and nitrogen on Vycor porous glass, *Proceedings of the Physical Society* 79 (855-868).  
URL <http://iopscience.iop.org/0370-1328/79/4/323>
- [68] J. H. Page, J. Liu, B. Abeles, E. Herbolzheimer, H. W. Deckman, D. A. Weitz, Adsorption and desorption of a wetting fluid in Vycor studied by acoustic and optical techniques, *Physical Review E* 52 (3) (1995) 2763–2777.  
URL <http://journals.aps.org/pre/abstract/10.1103/PhysRevE.52.2763>

- [69] J. C. Fisher, The fracture of liquids, *Journal of applied Physics* 19 (11) (1948) 1062–1067.
- [70] D. H. Trevena, *Cavitation and tension in liquids*, Adam Hilger, 1987.
- [71] D. W. Oxtoby, Homogeneous nucleation: theory and experiment, *Journal of Physics: Condensed Matter* 4 (38) (1992) 7627.
- [72] Q. Zheng, D. Durben, G. Wolf, C. Angell, Liquids at large negative pressures: water at the homogeneous nucleation limit, *Science* 254 (5033) (1991) 829–832.
- [73] V. I. Levitas, A. V. Idesman, A. K. Palakala, Phase-field modeling of fracture in liquid, *Journal of Applied Physics* 110 (3) (2011) 033531.
- [74] E. Masoero, M. Pinson, P. Bonnaud, H. Manzano, Q. Ji, S. Yip, J. Thomas, M. Bazant, K. Van Vliet, H. Jennings, Modelling hysteresis in the water sorption and drying shrinkage of cement paste, in: *CON-CREEP 10*, 2015, pp. 306–312.
- [75] H. M. Jennings, E. Masoero, M. B. Pinson, E. G. Strekalova, P. A. Bonnaud, H. Manzano, Q. Ji, J. J. Thomas, R. J.-M. Pellenq, F.-J. Ulm, et al., Water isotherms, shrinkage and creep of cement paste: hypotheses, models and experiments, in: *Mechanics and Physics of Creep, Shrinkage, and Durability of Concrete: A Tribute to Zdeňk P. Bažant*, 2013, pp. 134–141.
- [76] N. S. Martys, C. F. Ferraris, Capillary transport in mortars and concrete, *Cement and Concrete Research* 27 (5) (1997) 747–760.  
URL <http://www.sciencedirect.com/science/article/pii/S0008884697000525>
- [77] V. Baroghel-Bouny, Water vapour sorption experiments on hardened cementitious materials. Part II: Essential tool for assessment of transport properties and for durability prediction, *Cement and Concrete Research* 37 (3) (2007) 438–454. doi:10.1016/j.cemconres.2006.11.017.  
URL <http://linkinghub.elsevier.com/retrieve/pii/S0008884606003061>
- [78] P. Faucon, F. Adenot, J. F. Jacquinet, J. C. Petit, R. Cabrillac, M. Jorda, Long-term behaviour of cement pastes used for nuclear waste

- disposal: review of physico-chemical mechanisms of water degradation, *Cement and Concrete Research* 28 (6) (1998) 847–857.  
 URL <http://www.sciencedirect.com/science/article/pii/S0008884698000532>
- [79] E. Samson, J. Marchand, J. J. Beaudoin, Modeling the influence of chemical reactions on the mechanisms of ionic transport in porous materials: an overview, *Cement and Concrete Research* 30 (2000) 1895–1902.  
 URL <http://www.sciencedirect.com/science/article/pii/S0008884600004580>
- [80] F. P. Glasser, J. Marchand, E. Samson, Durability of concrete - Degradation phenomena involving detrimental chemical reactions, *Cement and Concrete Research* 38 (2) (2008) 226–246. doi:10.1016/j.cemconres.2007.09.015.  
 URL <http://linkinghub.elsevier.com/retrieve/pii/S0008884607002190>
- [81] J. Simunek, D. L. Suarez, Two-dimensional transport model for variably saturated porous media with major ion chemistry, *Water Resources Research* 30 (4) (1994) 1115–1133.  
 URL <http://onlinelibrary.wiley.com/doi/10.1029/93WR03347/full>
- [82] K. U. Mayer, E. O. Frind, D. W. Blowes, Multicomponent reactive transport modeling in variably saturated porous media using a generalized formulation for kinetically controlled reactions, *Water Resources Research* 38 (9) (2002) 13–1–13–21. doi:10.1029/2001WR000862.  
 URL <http://doi.wiley.com/10.1029/2001WR000862>
- [83] E. Masoero, G. Cusatis, G. Di Luzio, C–s–h gel densification: The impact of the nanoscale on self-desiccation and sorption isotherms, *Cement and Concrete Research* 109 (2018) 103–119.
- [84] D. Gawin, C. Majorana, B. Schrefler, Numerical analysis of hygro-thermal behaviour and damage of concrete at high temperature, *Mechanics of Cohesive-frictional Materials* 4 (1) (1999) 37–74.

- [85] C. T. Davie, C. J. Pearce, N. Bićanić, A fully generalised, coupled, multi-phase, hygro-thermo-mechanical model for concrete, *Materials and structures* 43 (1) (2010) 13–33.
- [86] G. Di Luzio, G. Cusatis, Hygro-thermo-chemical modeling of high performance concrete. i: Theory, *Cement and Concrete composites* 31 (5) (2009) 301–308.
- [87] O. F. Osanyintola, C. J. Simonson, Moisture buffering capacity of hygroscopic building materials: Experimental facilities and energy impact, *Energy and Buildings* 38 (10) (2006) 1270–1282. doi:10.1016/j.enbuild.2006.03.026.  
URL <http://linkinghub.elsevier.com/retrieve/pii/S0378778806000855>
- [88] M. Jerman, R. Černý, Effect of moisture content on heat and moisture transport and storage properties of thermal insulation materials, *Energy and Buildings* 53 (2012) 39–46. doi:10.1016/j.enbuild.2012.07.002.  
URL <http://linkinghub.elsevier.com/retrieve/pii/S0378778812003143>
- [89] C. Hall, M. Raymond Yau, Water movement in porous building material-IX. The water absorption and sorptivity of concretes, *Building and Environment* 22 (1) (1987) 77–82. doi:10.1016/0360-1323(87)90044-8.  
URL <http://linkinghub.elsevier.com/retrieve/pii/0360132387900448>
- [90] C. Hall, W. D. Hoff, S. C. Taylor, M. A. Wilson, B.-G. Yoon, H.-W. Reinhardt, M. Sosoro, P. Meredith, A. M. Donald, Water anomaly in capillary liquid absorption by cement-based materials, *Journal of Materials Science Letters* 14 (1995) 1178–1181.  
URL <http://www.springerlink.com/index/T83211M7719G3153.pdf>